

RSC Advances



This is an *Accepted Manuscript*, which has been through the Royal Society of Chemistry peer review process and has been accepted for publication.

Accepted Manuscripts are published online shortly after acceptance, before technical editing, formatting and proof reading. Using this free service, authors can make their results available to the community, in citable form, before we publish the edited article. This *Accepted Manuscript* will be replaced by the edited, formatted and paginated article as soon as this is available.

You can find more information about *Accepted Manuscripts* in the [Information for Authors](#).

Please note that technical editing may introduce minor changes to the text and/or graphics, which may alter content. The journal's standard [Terms & Conditions](#) and the [Ethical guidelines](#) still apply. In no event shall the Royal Society of Chemistry be held responsible for any errors or omissions in this *Accepted Manuscript* or any consequences arising from the use of any information it contains.

Cite this: DOI: 10.1039/c0xx00000x

www.rsc.org/xxxxxx

Enhancement of solar energy absorption using plasmonic nanofluid based on TiO₂/Ag composite nanoparticles

Yimin Xuan,^{*a,b} Huiling Duan^b and Qiang Li^b*Received (in XXX, XXX) Xth XXXXXXXXXX 20XX, Accepted Xth XXXXXXXXXX 20XX*

DOI: 10.1039/b000000x

Combined with solar irradiation spectrum, the optical properties of TiO₂/Ag composite nanoparticle and water-based nanofluids composed of different nanoparticles are both studied. The solar energy absorption features are compared among these nanofluids based on TiO₂, Ag and TiO₂/Ag composite nanoparticles. Due to localized surface plasmon resonance (LSPR) effect excited on Ag surface, the optical absorption of TiO₂/Ag plasmonic nanofluid is remarkably enhanced. The enhanced absorption property by LSPR excitation is introduced in solar thermal conversion. The photothermal experiments of different nanofluids conducted under the same condition reveal that TiO₂/Ag plasmonic nanofluid exhibits higher temperature compared with that of TiO₂ based nanofluid. Although the temperatures of Ag nanofluid and TiO₂/Ag nanofluid are equivalent, the cost of TiO₂/Ag based nanofluid is much lower. The effect of nanoparticle concentration on the photothermal performance of TiO₂/Ag plasmonic nanofluid is also studied in this paper.

1. Introduction

Solar energy is the most abundant energy in the world. Due to the more and more serious energy problem, the effective utilization of solar energy becomes especially important. Solar energy can be converted to many other energy forms, such as electricity, chemical energy and thermal energy. Among the three different forms of energy conversion, solar thermal collectors that utilize solar radiation to generate thermal energy are the most straightforward and simplest energy conversion equipment. The conventional solar thermal collector is a surface-based flat plate receiver, which harvests solar energy with a highly absorbing surface¹. Solar radiation is absorbed by the black surface and then transferred to the working fluid through convection and conduction. Therefore, the absorbing surface usually has a high temperature, which leads to significant radiative heat loss ($\propto T^4$), and consequently, lowers the overall conversion efficiency, especially for applications in the cases of concentrated solar collectors.

In order to decrease the heat loss at high temperature, Abdelrahman et al.² and Hunt³ proposed a black-liquid collector in the 1970s. In contrast to the surface-based solar thermal collector, solar energy is directly absorbed by the working fluid in black-liquid collector, so it is also called the volumetric solar thermal collector. Due to the absence of highly absorbing surface in a volumetric solar receiver, the surface temperature is much lower than that of surface based solar thermal collector, so that, the radiative heat loss can be reduced. Moreover, the overall thermal resistance is lowered since the thermal resistance from

hot absorbing surface to working fluid is eliminated^{4,5}.

For volumetric absorbers, the overall conversion efficiency is mainly limited by the optical absorption properties of working fluid. Therefore, in order to improve the photothermal performance of solar utilization, first of all, it is necessary to enhance the light absorption characteristics of working fluids. Recently, nanofluid (nano-sized particles suspended in base fluid) is introduced to solar thermal collectors as the working fluid that directly absorbs the solar irradiation. Nanoparticles offer the potential of improving the absorption properties of liquids, leading to an increase in the efficiency of photothermal performance. Taylor and co-workers⁶ compared the extinction coefficients of different nanofluids by model predictions and spectroscopic measurements. In their study, over 95% of incoming light can be absorbed with low nanoparticle volume fraction. Otanicar et al.⁷ examined the photothermal efficiencies of nanofluids made from a variety of nanoparticles (carbon nanotubes, graphite, and silver). By controlling the size, shape, material, and volume fraction of the nanoparticles, the absorption spectrum can be tuned to maximize absorption of solar energy. The efficiency improvement of up to 5% was achieved using nanofluids as the absorption mechanism. Saidur and co-workers⁸ analyzed the effect of nanofluid on the efficiency of direct solar collector, and investigated the absorption properties of aluminum nanofluid by varying the particle size and volume fraction. With only 1% volume fraction, the aluminum nanofluid is almost opaque to light, and the efficiency improvement is promising.

Metal nanoparticles can excite localized surface plasmon resonance (LSPR) effects on their surfaces⁹⁻¹². This resonant

effect is excited when oscillation frequency of electrons is consistent with the incident light frequency. At resonance frequency, both the near electric-field properties and far-field absorption properties are strongly enhanced¹³⁻¹⁶. Therefore, combination of the LSPR effect of some noble metallic nanoparticles and the technique of nanofluids leads to a new concept of plasmonic nanofluid. As the name implies, the plasmonic nanofluid is composed of plasmonic nanoparticles and base liquid. This new type of nanofluid can be used as working fluid in volumetric solar thermal collectors to enhance light absorption by means of the LSPR effect of the plasmonic nanoparticles suspended in the base fluid. Our previous work examined the absorption properties of plasmonic core/shell nanoparticle suspensions and theoretically revealed their potential application for solar energy harvesting¹⁷. Compared with nanoparticles of single component, the plasmonic composite nanoparticles have many advantages, such as enhanced absorption of light and tuneable resonance frequency and intensity. The volumetric solar thermal receivers based on nanoparticles with single-component are widely studied. However, there are fewer studies on nanofluid solar thermal collectors based on plasmonic nanostructures. Lee et al.¹ theoretically studied the feasibility of a plasmonic nanofluid-based solar collection to enhance broad-band solar thermal absorption.

To improve the photothermal efficiency of nanofluid-based solar thermal collector, the most important thing is to enhance optical absorption of nanofluid, which is affected by intrinsic optical properties of nanoparticles and their volume concentration¹. In this paper, we prepare plasmonic hybrid nanoparticles and plasmonic nanofluids to experimentally explore the feasibility of making use of the localized surface plasmon resonance (LSPR) effect to enhance solar thermal absorption. The optical properties of TiO₂/Ag composite nanoparticles and their suspension system are studied. Then, the photothermal performance of TiO₂/Ag nanofluid is examined under solar light irradiation and compared with other nanofluids.

2. Plasmon resonance effect

Under the illumination of incident light, the conductive electrons in metal core are driven by the restoring force. If the oscillation frequency of electrons matches with the frequency of incident light, a plasmon resonance can arise⁹. The resonance modes excited on conductive nanoparticle surface are called localized surface plasmon resonance (LSPR). It can be excited by direct light illumination. The excitation of LSPR effect is wavelength-dependent. In the electrostatic approximation, the complex polarizability α of a small nanoparticle of sub-wavelength diameter can be expressed as⁹:

$$\alpha = 4\pi R^3 \frac{\varepsilon - \varepsilon_m}{\varepsilon + 2\varepsilon_m} \quad (1)$$

where R is the particle radius, ε and ε_m are the dielectric constants of the particle and environment respectively. It can be observed that the polarizability α can be resonantly enhanced if the denominator $|\varepsilon + 2\varepsilon_m|$ is a minimum. The condition that satisfies $\text{Re}[\varepsilon(\omega)] + 2\varepsilon_m = 0$ is called Fröhlich condition, under which the

plasmon resonance can be excited.

When LSPR effect is excited, an enhancement of light absorption and scattering at wavelengths corresponding to their plasmon resonance can be achieved. LSPR effect can localize energy in the vicinity of metals, leading to electric field around the metal nanostructure strongly enhanced. So that, based on the LSPR effect excited on metal surface, the plasmonic nanostructures can be used to harvest solar energy for a variety of applications, such as solar cells, solar thermal collectors, photocatalytic applications and so on.

The resonance wavelength is dependent on particle shape, size and environment. By controlling the particle size, both the resonance wavelength and intensity can be tuned in a wide range of wavelengths^{10, 18}. Therefore, the spectrum can be selectively controlled by the utilization of LSPR effect. By combining plasmonic nanostructures of different sizes and shapes, a broadband absorption spectrum may be obtained. Cole and Halas¹⁹ determined the ideal distributions of spherical metallic nanoparticles to fit the solar spectrum at the earth's surface. Lv and co-workers²⁰ investigated the wavelength tuning ranges for different metallic shell nanoparticle and revealed that efficient spectral solar absorption fluids can be obtained using core/shell plasmonic nanoparticle suspensions. Based on LSPR effect, it is possible to design plasmonic nanostructures used in applications that require variable spectral absorption or scattering. In this paper, the plasmonic nanoshells are used in photothermal areas. Due to LSPR effect excited on plasmonic nanoshells, a great enhancement of optical absorption is achieved.

3. Theoretical Models

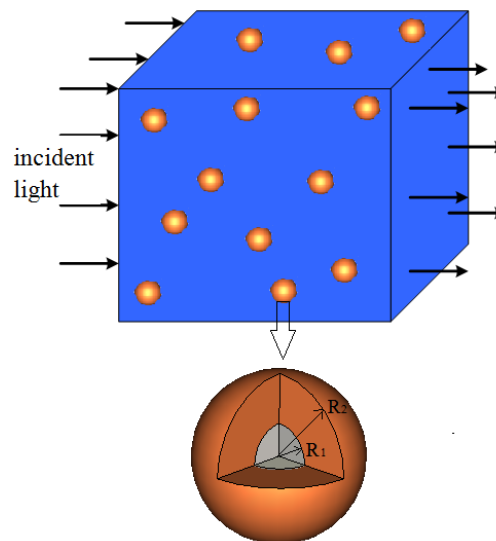


Fig. 1 Schematic of the core/shell suspension system, nanoparticles are randomly dispersed in water.

Schematic of the core/shell suspension system is shown in Figure 1. The composite nanostructures made of TiO₂ core and Ag shell are dispersed randomly in water. It is known that photothermal performance is determined by the optical absorption of nanofluid. So, the optical properties of nanoparticles and nanofluid both have to be examined.

3.1 Model of nanoparticles

In this study, the nanoparticles are assumed to be spherical, so their optical properties can be conveniently simulated based on Mie's theory. This method expands the internal and scattered fields into a set of normal modes described by vector harmonics. After a series of derivation, the scattering and extinction cross sections can be given by the following relation²¹:

$$C_{sca} = \frac{W_s}{I_i} = \frac{2\pi}{k^2} \sum_{n=1}^{\infty} (2n+1)(|a_n|^2 + |b_n|^2) \quad (2)$$

$$C_{ext} = \frac{W_{ext}}{I_i} = \frac{2\pi}{k^2} \sum_{n=1}^{\infty} (2n+1) \text{Re}(a_n + b_n) \quad (3)$$

Absorption cross section can be obtained using:

$$C_{abs} = C_{ext} - C_{sca} \quad (4)$$

where C_{sca} , C_{ext} and C_{abs} are scattering, extinction and absorption cross sections, k is wave number, a_n and b_n are scattering coefficients for core/shell nanoparticle by considering the interference between forwardly and backwardly propagating spherical waves²².

The scattering and absorption cross sections are quantities about area, which are functions of particle size. Generally, scattering and absorption are evaluated by dimensionless efficiency factors Q_{sca} and Q_{abs} respectively. They are defined as the ratio of scattering or absorption cross sections to geometrical cross section, as shown below:

$$Q_{sca} = \frac{C_{sca}}{\pi R_2^2} \quad (5)$$

$$Q_{abs} = \frac{C_{abs}}{\pi R_2^2} \quad (6)$$

The dielectric constants of Ag and TiO₂ materials are wavelength-dependent, which are obtained from reference²³. The refractive index for water obtained from reference²⁴ is also dependent upon wavelength in near infrared region.

3.2 Model of nanofluid

For the purpose of fully understanding the effects of suspended nanoparticles in a base fluid, the complete optical properties of nanofluid are needed. Water is a normally used base fluid in solar thermal application since it is non-toxic, however, its absorption is weak²⁵. By suspending nanoparticles in it, the optical absorption can be improved. In this study, we suspend TiO₂/Ag nanoparticles in water composing plasmonic nanofluid. The suspension system is shown in Figure 1. Most of the available studies neglect the interactions between nanoparticles. They assume that the scattering from nanoparticles is independent. But, when concentration is great, interactions between nanoparticles may be significant. Especially for the plasmonic nanoparticle suspension system, both absorption and scattering are enhanced greatly as LSPR effect is excited. Light scattered from one particle may be utilized by others, so that their interactions have to be taken into account.

In this work, finite difference time domain (FDTD) method is used to simulate the optical properties of TiO₂/Ag nanofluid. This

method is an explicit time marching algorithm used to solve Maxwell's curl equations on discretized spatial grids²⁶. Based on this method, the propagation of electromagnetic waves within suspension system can be simulated, so that inter-particle coupling inside nanofluid is involved during computation. The electromagnetic propagation in nanofluid can be described by the Maxwell's equations:

$$\varepsilon \frac{\partial \vec{E}}{\partial t} = \nabla \times \vec{H} - \vec{J} \quad (7)$$

$$\mu \frac{\partial \vec{H}}{\partial t} = -\nabla \times \vec{E} \quad (8)$$

$$\vec{J} = \sigma \vec{E} \quad (9)$$

where E and H are electric and magnetic fields, ε and μ are permittivity and permeability of medium, J is current density, and σ is conductivity.

These equations are solved on the discrete grids by replacing all the derivatives with finite-difference expressions. The discretization of the computational domain is usually based on Yee grid²⁷. Both the near-field and far-field properties can be conveniently calculated by this method. The reflection and transmission energies can be determined by Poynting theorem:

$$\vec{S}_{ref} = \frac{1}{2} \text{Re}[\vec{E}_{ref} \times \vec{H}_{ref}^*] \quad (10)$$

$$\vec{S}_{tr} = \frac{1}{2} \text{Re}[\vec{E}_{tr} \times \vec{H}_{tr}^*] \quad (11)$$

where S_{ref} and S_{tr} are the time-averaged Poynting vectors corresponding to the reflected and transmission waves. Perfectly matched layers (PML) are imposed at the left and right surfaces along light incident direction to absorb nearly all the incident waves. At other surfaces, periodic boundary conditions are imposed. The volume concentration of nanoparticle suspension system is defined in the following form:

$$f = \frac{4N\pi R^3}{3V_{total}} \quad (12)$$

where N is the number of particles suspended in water.

4. Experimental Section

4.1 Preparation of TiO₂/Ag plasmonic nanofluid

The plasmonic nanofluid was prepared by two steps. First, TiO₂/Ag composite nanoparticles had to be prepared. TiO₂ powders were provided by Deke Technology Company. According to reference²⁸, TiO₂/Ag composite nanoparticles were synthesized by photo-chemical impregnation method. Ag nanoparticles were deposited on TiO₂ surface like islands. Then, TiO₂/Ag plasmonic nanofluid was prepared by adding certain amount of the prepared composite nanoparticles to base fluid. In order to make TiO₂/Ag nanoparticles uniformly dispersed in base fluid, the dispersion system needed to be sonicated sufficiently.

4.2 Experimental setup

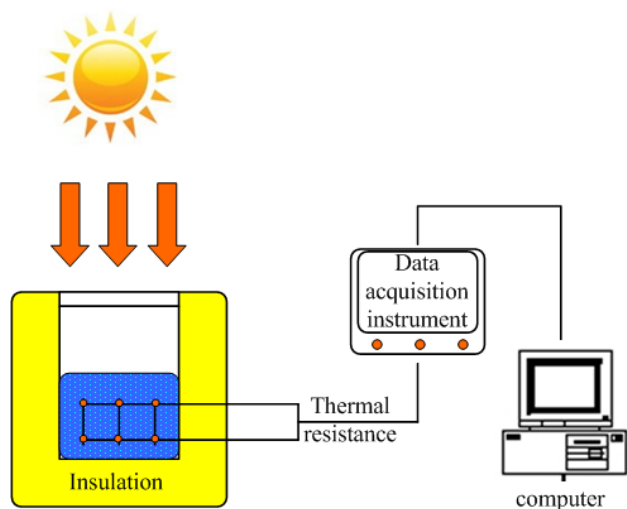


Fig. 2 Schematic of the experimental setup for solar thermal conversion

In this paper, the effect of concentration on photothermal performance of TiO_2/Ag plasmonic nanofluid is investigated experimentally. The schematic of experimental setup is shown in Figure 2. The size of nanofluid container is $60 \times 60 \times 80 \text{ mm}^3$ with square bottom surface. This container is made of glass and is coated with insulation materials except for the top surface. The top surface is covered with a transparent glass. Sunlight is transmitted through the glass cover, then, absorbed by TiO_2/Ag

nanofluid. The temperature sensor is chosen as Measurement thermistor model 10K3MCD1 whose sizes are 3.3 mm long and 0.48 mm in diameter with a nominal resistance of 10 k Ω at 25 $^\circ\text{C}$. They are located at different depths and different positions in nanofluid. The average value is taken as the mean temperature of nanofluid. The resistances of thermistor are measured using a Keithly model 2700 multimeter equipped with an 80-channel scanner by employing precise four-wire resistance measurements and low excitation current to minimize the thermistor self-heating. The resistance of thermistor is a function of temperature, by a simple mathematical conversion, the temperatures can be obtained. Solar irradiance intensity measured by TES 1333R Solar Power Meter is recorded every minute.

The photothermal efficiency η can be estimated by:

$$\eta = \frac{mc_p(T_f - T_i)}{AG\Delta t} \quad (13)$$

where m is the mass of nanofluid, c_p is the specific heat of nanofluid measured by Mettler Toledo DSC1 STAR^e System, T_i is initial temperature, T_f is final temperature, A is the top surface area of receiver, G is the incident solar heat flux, Δt is the time exposed to solar radiation.

5. Results and Discussion

5.1 Optical properties of nanoparticles

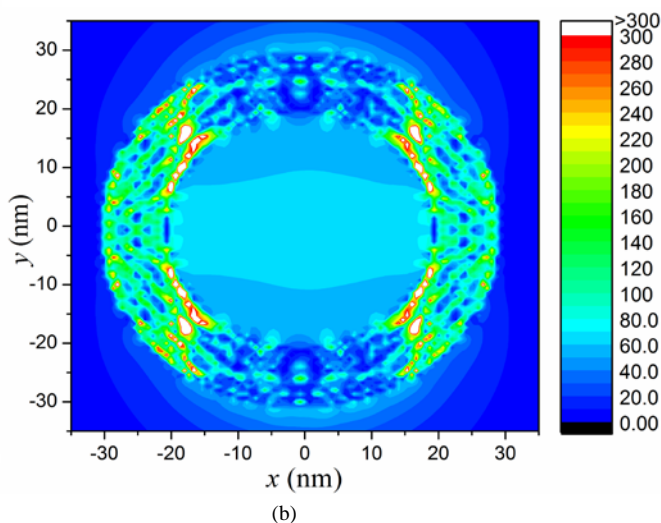
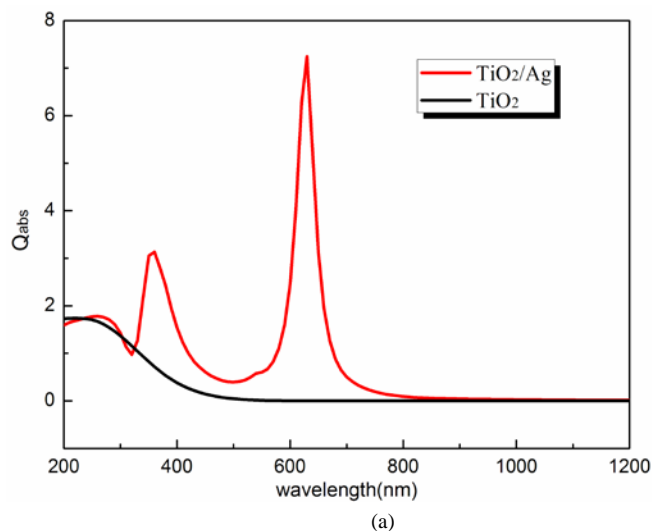


Fig. 3 (a) Absorption efficiency Q_{abs} of TiO_2/Ag core/shell nanoparticle and solid TiO_2 nanoparticle. (b) Electric field around TiO_2/Ag nanoparticle at $\lambda = 630 \text{ nm}$. These results are obtained from the numerical simulation.

In order to obtain an improvement of overall photothermal performance, the suspended nanoparticles have to be fine absorbers of incident solar energy. TiO_2/Ag composite nanoparticle is studied in this work due to its unique optical properties. The simulated optical absorption of TiO_2 nanoparticle with $R = 30 \text{ nm}$ and that of TiO_2/Ag core/shell nanoparticle with $R_1/R_2 = 20/30 \text{ nm}$ are shown in Figure 3(a).

Compared with solid TiO_2 nanoparticles, TiO_2/Ag composite nanoparticle exhibits an enhanced optical absorption. It is caused by the localized surface plasmon resonance (LSPR) effect excited on Ag surface. LSPR is a resonant effect that originates from the

collective oscillation of conductive electrons in metals. The collective oscillation efficiency is called resonance frequency. As shown in Figure 3(a), two obvious resonance peaks can be observed at wavelengths 360 nm and 630 nm. The electric field is greatly strengthened in Ag shell at resonance wavelength (as shown in Figure 3(b)), so that a remarkable enhancement of optical absorption can be obtained²⁹.

The resonance frequency and intensity are dependent on the core and shell sizes. This sensitive dependence arises from the hybridization interaction between the plasmons of inner and outer metallic interfaces of the nanoshell^{19, 30}. Figure 4 shows the

spectral solar irradiance and absorption spectra of TiO₂/Ag nanoparticles with different core size. It can be observed that the solar irradiance is strongest in the visible light region. As core size increases, the resonance peak is red shifted, which gradually deviates from the strongest solar irradiance region. For the purpose of utilizing solar energy efficiently, the absorption spectra of nanoparticles should fit the solar spectrum at the earth's surface. As shown in Figure 4, the absorption peak of TiO₂/Ag nanoparticle with $R_1/R_2 = 25/30$ nm is strongest than that of nanoparticles with other core sizes. However, its resonance wavelength is located at 840 nm where the solar irradiance is weaker. Although, the absorption peak of TiO₂/Ag nanoparticle with $R_1/R_2 = 20/30$ nm is weaker than that of nanoparticle with $R_1/R_2 = 25/30$ nm, the plasmon resonance excited at 630 nm lies in the region where solar irradiance is strong. Therefore, for the core/shell nanoparticles with $R_1 = 20$ nm and $R_1 = 25$ nm, it is difficult to determine the preferred core size whose overall absorption of solar light is stronger from Figure 4.

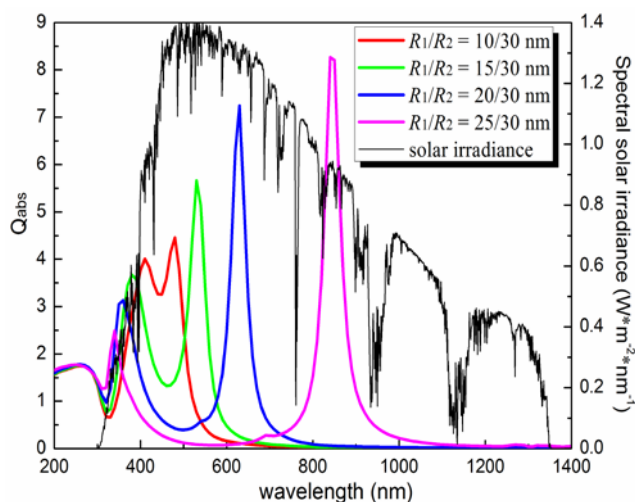


Fig. 4 Absorption efficiency Q_{abs} of TiO₂/Ag core/shell nanoparticles with different core size, spectral solar irradiance is also presented

The above analysis shows that TiO₂/Ag composite nanoparticle is an excellent optical absorber. Due to the LSPR effect excited on Ag surface, the optical absorption is greatly enhanced. However, for nanofluid-based solar thermal application, the nanoparticles are randomly dispersed in base fluid, so that the optical properties of nanofluid are also affected by nanoparticle concentration as well as interactions among nanoparticles. Therefore, besides the optical properties of single nanoparticle, the overall optical properties of TiO₂/Ag plasmonic nanoparticle suspension system also need to be discussed. In section 4.2, the absorbed solar energy is compared between nanofluids with core size $R_1 = 20$ nm and $R_1 = 25$ nm. According to the overall absorbed energy, the preferred core size can be determined. The effect of concentration on overall absorption is discussed based on the nanoparticles with preferred sizes.

5.2 Optical properties of nanofluid

To determine the effectiveness of nanofluids in solar applications, their absorption of the solar energy must be established. The effect of nanoparticle material on overall absorbance is shown in Figure 5. The optical absorption of nanofluids based on TiO₂, Ag

and TiO₂/Ag composite nanoparticles are compared. They are studied under the condition of same volume fraction $f = 0.01$. It can be observed that TiO₂ nanofluid mainly absorb the UV light in the region where solar irradiance is rather weak.

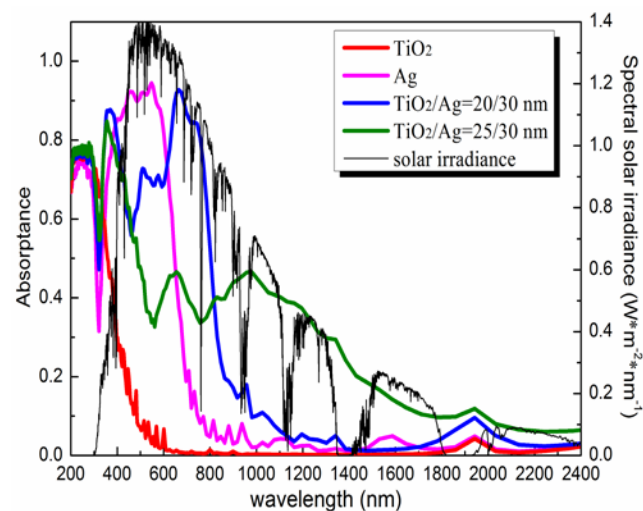


Fig. 5 Absorbance of nanofluids based on different nanoparticles (Ag, TiO₂ and TiO₂/Ag core/shell), solar spectrum is also presented

Compared with TiO₂ nanofluid, the absorption spectrum of Ag nanofluid is extended, which is mainly in the UV and visible light region. So, obviously, the absorption performance of Ag nanofluid is better than that of TiO₂ nanofluid. For nanofluid based on TiO₂/Ag composite nanoparticles, the absorption spectrum is further extended to longer wavelengths. As the core size increases from 20 nm to 25 nm, the absorption spectrum is broadened. This TiO₂/Ag plasmonic nanofluid can absorb light in a wide range of wavelengths (from UV to near infrared). The curves in Fig. 5 imply that by selecting proper fractions of TiO₂/Ag hybrid nanoparticles with different sizes, one can enhance the absorption performance of plasmonic nanofluids within the near- and mid-infrared wavelength ranges.

Therefore, to compare the absorption performance of different nanofluids, the solar energy absorbed should be determined. The energy absorbed by nanofluid can be obtained from the following equation:

$$G_a = \int_{\lambda_1}^{\lambda_2} G_s(\lambda) * A(\lambda) d\lambda \quad (14)$$

where G_a is the energy absorbed by nanofluid, $G_s(\lambda)$ is the spectral solar irradiance, $A(\lambda)$ is absorbance of nanofluid.

Table 1 Absorbed energy G_a by different nanofluid

nanofluid	energy absorbed G_a (W/m ²)
TiO ₂	57.89072
Ag	390.8815
TiO ₂ /Ag (20/30 nm)	484.9153
TiO ₂ /Ag (25/30 nm)	413.3601

The integrated solar energies absorbed by different nanofluids are shown in Table 1. Among the four kinds of nanofluids, TiO₂/Ag nanofluid with $R_1/R_2 = 20/30$ nm absorbs the most energy than others. Accordingly, the overall absorption of

nanofluid based on TiO₂/Ag composite nanoparticles is superior to that of TiO₂ or Ag nanofluid. Moreover, the energy absorbed by TiO₂/Ag nanofluid with core size $R_1 = 20$ nm is larger than that with $R_1 = 25$ nm. Therefore, in the following discussion, the effects of volume fraction on overall absorption properties are explored based on TiO₂/Ag nanoparticles with $R_1/R_2 = 20/30$ nm.

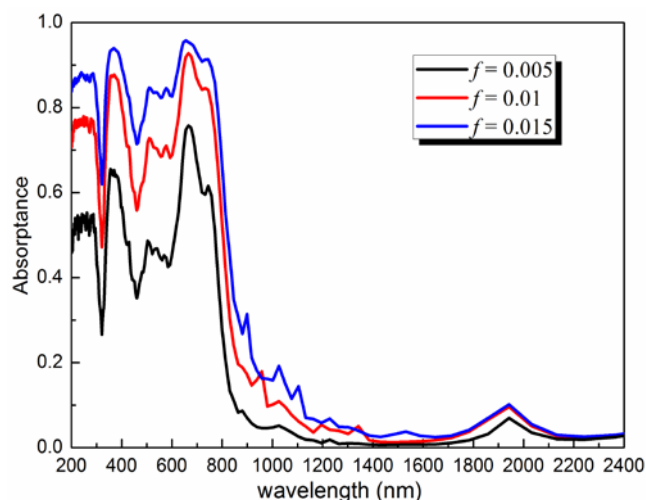


Fig. 6 Optical absorbance of TiO₂/Ag nanofluid as a function of volume fraction

The effect of volume fraction on optical absorbance of TiO₂/Ag nanofluid is shown in Figure 6. It can be observed that TiO₂/Ag nanofluid mainly absorbs UV-visible light which accounts for about 47% of solar irradiation energy³¹. As volume fraction f increases, the absorbance of TiO₂/Ag based nanofluid is gradually improved. When f varies from 0.005 to 0.01, the maximal absorbance can increase from 0.757 to 0.928. The interactions among suspended nanoparticles are affected by nanoparticle concentration. More nanoparticles give rise to multi-scattering within the dispersion system and cause longer optical paths inside it. Then, an enhanced light absorption can be obtained. Further increasing volume fraction f to 0.015, the optical absorbance improves a little. Therefore, an optimal volume fraction maybe exists. Under the optimal volume fraction, the optical absorption of nanofluid may be saturated. Further increasing volume fraction, the absorption spectrum changes a little.

5.3 Photothermal performance of TiO₂/Ag nanofluid

The nanofluids based on Ag, TiO₂, and TiO₂/Ag composite nanoparticles are irradiated by solar light. They have the same volume fraction $f = 0.005$. Temperatures of these nanofluids are measured under the same condition. Figure 7 shows the temperatures of different nanofluids varying with time.

Under solar light irradiation, the temperatures of nanofluid gradually increase with time. As solar radiation intensity weakens, the nanofluid temperatures also gradually decrease. Obviously, due to the optical absorption of nanoparticles, the temperatures of nanofluids are higher than that of deionized water. The maximal temperature of nanofluid based on TiO₂/Ag composite nanoparticles is equivalent to that of Ag nanofluid. It is much higher than the temperature of TiO₂ nanofluid, because the energy absorbed by TiO₂/Ag plasmonic nanofluid is much more than that absorbed by TiO₂ nanofluid (as shown in Figure 5). Although the temperatures of TiO₂/Ag nanofluid and Ag nanofluid are equivalent, the cost of TiO₂/Ag nanofluid is lower than that of Ag nanofluid, since the noble metal Ag used in TiO₂/Ag nanofluid is less than that used in Ag nanofluid under the same volume fraction.

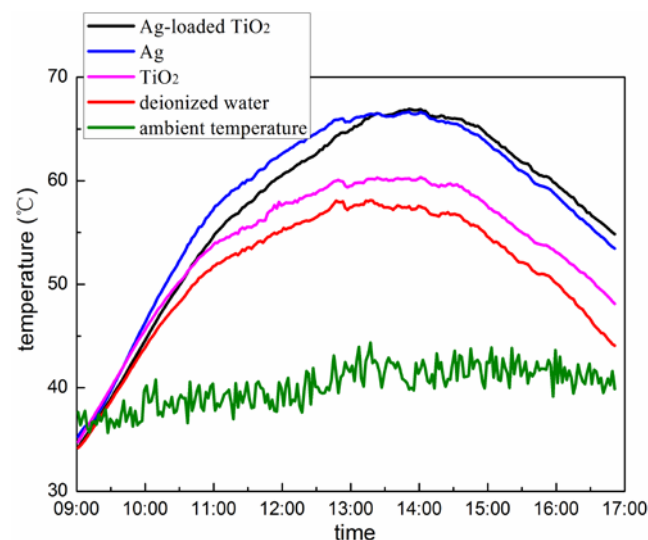


Fig. 7 Temperatures of different nanofluids as a function of time ($f = 0.005$)

Table 2 Photothermal efficiencies of nanofluids based on TiO₂, Ag and TiO₂/Ag nanoparticles as well as deionized water

nanofluid	average solar irradiation G (W/m ²)	specific heat c_p (J/g·K)	Maximal temperature T_f (°C)	photothermal efficiency η (%)
TiO ₂	1004.122	3.89	60.21	16.07
Ag	1004.122	4.035	66.65	20.86
Ag-loaded TiO ₂ ($f = 0.005$)	1004.122	4.01	66.93	20.9
deionized water	1004.122	4.2	57.52	15.52

The photothermal conversion experiment based on different nanofluids is performed under the same solar irradiation and volume fraction. Photothermal efficiency can be estimated from equation (12). Table 2 shows the thermophysical properties of

various nanofluids, solar irradiation intensity as well as their corresponding photothermal efficiencies. Obviously, the photothermal efficiencies of nanofluids are higher than that of water without nanoparticles. The photothermal efficiency of

nanofluid based on TiO₂/Ag nanoparticles is near to that of Ag nanofluid. It shows that their absorption performance is equivalent. However, TiO₂/Ag nanofluid has cost advantages.

5.4 Effect of concentration on photothermal performance

5 Due to the strong absorption of TiO₂/Ag composite nanoparticles, their corresponding nanofluid exhibits benign photothermal performance. The effect of concentration on photothermal performance is studied based on TiO₂/Ag nanofluid. Under the same solar irradiation, the variation of temperature with time is measured for different volume fraction (as shown in Figure 8).
10 Among the four volume fractions examined, it can be observed that the temperature of nanofluid increases with volume fraction when $f < 0.01$, which is easy to be understood. The amount of nanoparticles suspended in water increases with concentration, so that more light can be confined in suspension system. The nanofluid with $f = 0.01$ exhibits the highest temperature. However, further increasing volume fraction to 0.015, the temperature decreases. As the simulation results shown in Figure 6, the optical absorption of the nanofluid somewhat improves when volume
20 fraction increases to 0.015. The absorption of light is almost saturated when volume fraction further increases. Moreover, for nanofluid of high concentration, solar energy is mainly absorbed in a very short depth near the surface³². The inner layers are not directly heated by light, which is similar to the surface based
25 solar thermal collector, leading to a great heat loss from the hot surface.

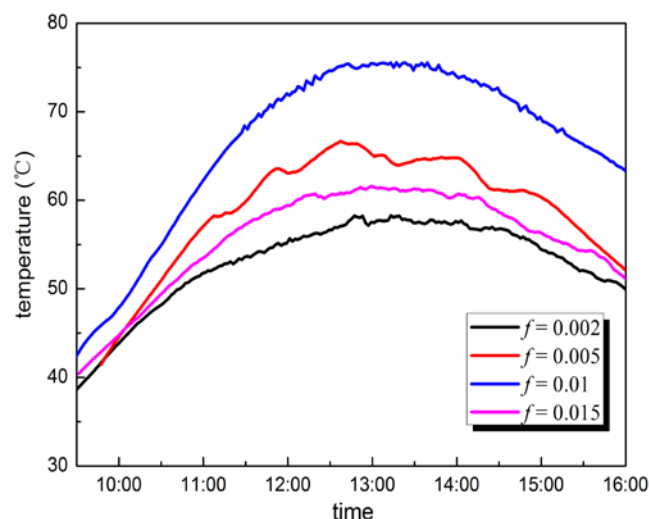


Fig. 8 Temperatures of TiO₂/Ag nanofluids with different concentration varies with time

6. Conclusion

30 The feasibility of using plasmonic nanofluid has been experimentally explored. The TiO₂/Ag plasmonic nanofluid has been prepared by dispersing TiO₂/Ag composite nanoparticles in water. The optical properties of TiO₂/Ag nanoparticle and
35 nanofluid have been studied, which indicates that TiO₂/Ag plasmonic nanoparticle is an admirable light absorber due to the LSPR effect excited on Ag surface. In addition, the photothermal conversion experiments have been performed for several different nanofluids. The temperature of TiO₂/Ag plasmonic nanofluid is

40 much higher than that of TiO₂ nanofluid under the same incident intensity. Although the temperature of TiO₂/Ag nanofluid is equivalent to that of Ag nanofluid, the nanofluid based on TiO₂/Ag composite nanoparticles has cost advantage. TiO₂/Ag plasmonic nanofluid of eminent photothermal property has
45 potential applications in volumetric solar thermal receivers.

Acknowledgments

This work was financially supported by the National Natural Science Foundation of China (Grant No. 50936002) and the 333 scientific research project of Jiangsu province (Grant
50 No. BRA2011134). The authors thank Dr. Ping Zhang for his help with experiment.

Notes and references

- ^a School of Energy and Power Engineering, Nanjing University of Aeronautics and Astronautics, Nanjing 210016, China. Fax: +86 25 84890688; Tel: +86 25 84891512; E-mail: ymxuan@nuaa.edu.cn
- ^b School of Energy and Power Engineering, Nanjing University of Science and Technology, Nanjing 210094, China.
1. B. J. Lee, K. Park, T. Walsh and L. Xu, *J. Sol. Energy Eng.*, 2012, 134, 021009.
2. M. Abdelrahman, P. Fumeaux and P. Suter, *Sol. Energy*, 1979, 22, 45-48.
3. A. J. Hunt, *Small particle heat exchangers*, Lawrence Berkeley National Laboratory, 1978.
4. T. P. Otanicar, *Enhancing the heat transfer in energy systems from a volumetric approach*, Hawaii, 2011.
5. R. A. Taylor, P. E. Phelan, T. P. Otanicar, C. A. Walker, M. Nguyen, S. Trimble and R. Prashe, *Renewable Sustainable Energy Rev.*, 2011, 3, 023104.
6. R. A. Taylor, P. E. Phelan, T. P. Otanicar, R. Adrian and R. Prasher, *Nanoscale Res. Lett.*, 2011, 6, 225/221-225/211.
7. T. P. Otanicar, P. E. Phelan, R. S. Prasher, G. Rosengarten and R. A. Taylor, *J. Renewable Sustainable Energy*, 2010, 2, 033102.
8. R. Saidur, T. C. Meng, Z. Said, M. Hasanuzzaman and A. Kamyar, *Int. J. Heat Mass Transfer*, 2012, 55, 5899-5907.
9. S. A. Maier, *Plasmonics: Fundamentals and applications*, Springer, New York, 2006.
10. C. Noguez, *J. Phys. Chem. C*, 2007, 111, 3806-3819.
11. J. Yao, A.-P. Le, S. K. Gray, J. S. Moore, J. A. Rogers and R. G. Nuzzo, *Adv. Mater.*, 2010, 22, 1102-1110.
12. Y. Hu, R. C. Fleming and R. A. Drezek, *Opt. Express*, 2008, 16, 19579-19591.
13. S. C. Warren and E. Thimsen, *Energy Environ. Sci.*, 2012, 5, 5133-5146.
14. Y. Zhao and C. Burda, *Energy Environ. Sci.*, 2012, 5, 5564-5576.
15. S. Chang, Q. Li, X. Xiao, K. Y. Wong and T. Chen, *Energy Environ. Sci.*, 2012, 5, 9444-9448.
16. W. Hou, P. Pavaskar, Z. Liu, J. Theiss, M. Aykol and S. B. Cronin, *Energy Environ. Sci.*, 2011, 4, 4650-4655.
17. H. Duan and Y. Xuan, *Appl. Energy*, 2014, 114, 22-29.
18. K. L. Kelly, E. Coronado, L. L. Zhao and G. C. Schatz, *J. Phys. Chem. B*, 2003, 107, 668-677.
19. J. R. Cole and N. J. Halas, *Appl. Phys. Lett.*, 2006, 89, 153120/153121-153120/153123.
20. W. Lv, P. E. Phelan, R. Swaminathan, T. P. Otanicar and R. A. Taylor, *J. Sol. Energy Eng.*, 2013, 135, 021005.
21. C. F. Bohren and D. R. Huffman, *Absorption and Scattering of Light by Small Particles*, John Wiley & Sons, Inc, New York, 1998.
22. D. D. Smith and K. A. Fuller, *J. Opt. Soc. Am. B*, 2002, 19, 2449-2455.
23. D. E. Palik, *Handbook of Optical Constants of Solids*, Academic Press Inc, London, 1985.
24. G. M. Hale and M. R. Querry, *Appl. Opt.*, 1973, 12, 555-563.

-
25. T. P. Otanicar, P. E. Phelan and J. S. Golden, *Sol. Energy*, 2009, 83, 969-977.
 26. C. Oubre and P. Nordlander, *J. Phys. Chem. B*, 2004, 108, 17740-17747.
 - 5 27. K. S. Yee, *IEEE Trans. Antennas Propag.*, 1966, 14, 302-307.
 28. S. X. Liu, Z. P. Qu, X. W. Han and C. L. Sun, *Catal. Today*, 2004, 93, 877-884.
 29. V. E. Ferry, A. Polman and H. A. Atwater, *ACSNano*, 2011, 5, 10055-10064.
 - 10 30. E. Prodan and P. Nordlander, *J. Chem. Phys.*, 2004, 120, 5444-5454.
 31. Q. Li, B. Guo, J. Yu, J. Ran, B. Zhang, H. Yan and J. R. Gong, *J. Am. Chem. Soc.*, 2011, 133, 10878-10884.
 32. E. Sani, S. Barison, C. Pagura, L. Mercatelli, P. Sansoni, D. Fontani, D. Jafrancesco and F. Francini, *Opt. Express*, 2010, 18, 5179-5187.